

PAPER

## New developments in isotropic turbulent models for FENE-P fluids

To cite this article: P R Resende and A S Cavadas 2018 *Fluid Dyn. Res.* **50** 025508

View the [article online](#) for updates and enhancements.

# New developments in isotropic turbulent models for FENE-P fluids

P R Resende<sup>1</sup> and A S Cavadas<sup>2</sup>

<sup>1</sup> São Paulo State University (Unesp), Institute of Science and Technology, Sorocaba, Brazil

<sup>2</sup> UIDM, ESTG, Polytechnique Institute of Viana do Castelo, Viana do Castelo, Portugal

E-mail: [resende@sorocaba.unesp.br](mailto:resende@sorocaba.unesp.br)

Received 12 August 2016, revised 18 October 2017

Accepted for publication 29 November 2017

Published 29 January 2018



CrossMark

Communicated by Yasuhide Fukumoto

## Abstract

The evolution of viscoelastic turbulent models, in the last years, has been significant due to the direct numeric simulation (DNS) advances, which allowed us to capture in detail the evolution of the viscoelastic effects and the development of viscoelastic closures. New viscoelastic closures are proposed for viscoelastic fluids described by the finitely extensible nonlinear elastic-Peterlin constitutive model. One of the viscoelastic closure developed in the context of isotropic turbulent models, consists in a modification of the turbulent viscosity to include an elastic effect, capable of predicting, with good accuracy, the behaviour for different drag reductions. Another viscoelastic closure essential to predict drag reduction relates the viscoelastic term involving velocity and the tensor conformation fluctuations. The DNS data show the high impact of this term to predict correctly the drag reduction, and for this reason is proposed a simpler closure capable of predicting the viscoelastic behaviour with good performance. In addition, a new relation is developed to predict the drag reduction, quantity based on the trace of the tensor conformation at the wall, eliminating the need of the typically parameters of Weissenberg and Reynolds numbers, which depend on the friction velocity. This allows future developments for complex geometries.

Keywords: isotropic turbulent models, viscoelastic fluids, FENE-P model

(Some figures may appear in colour only in the online journal)

## 1. Introduction

The first turbulence models for viscoelastic fluids to consider the elastic component were developed by Pinho (2003), Cruz *et al* (2004), Resende *et al* (2006). These models were

based primarily on a modified generalized Newtonian fluid (GNF) constitutive equation for the rheology representation, and then were modified ad-hoc to incorporate the elastic contribution in turbulent flow through the third invariant of the rate of deformation tensor. Therefore, there are limitations in the predictions of velocity field and also of the kinetic turbulent energy as the drag reduction is increased. This limitations are also seen in turbulence model of the second order type, as referenced by Resende *et al* (2013a). This occurs because the GNF constitutive equation is not a truly viscoelastic equation like the FENE-P model as it does not contain a memory effect.

The viscoelastic turbulent models mentioned before were developed using experimental data without detailed information, but with the powerful computational advances, it was possible to obtain full information about the elastic effect for the different drag reduction regimes, due to the DNS research on turbulent flows with non-Newtonian fluids.

Direct numerical simulations (DNS) of turbulent channel flow of homogeneous polymer solutions allowed to understand various aspects of the drag reduction phenomenon by investigating the effects of rheological parameters on DR mechanisms.

Most of the studies in literature in wall-bounded viscoelastic turbulence investigate the effect of increasing the polymer relaxation time and achieving maximum drag reduction.

One exception is the work of Dubief *et al* (2013) which endeavours in relating maximum drag reduction in wall-bounded viscoelastic turbulence with elasto-inertial turbulence (EIT) which is precisely characterized by strong turbulence-polymer interactions. The comprehension of these interaction is essential to develop models of the sub-grid stress for large-eddy-simulations of viscoelastic flows. The term EIT is due to a strong interaction between the inertial and the elastic degrees of freedom, which occurs when the maximum drag reduction is observed, i.e., when the relaxation time of the polymer solution is large with respect to the turbulence time scales and the shear time scale imposed by the wall.

Most of DNS simulations have used constitutive equations based on the finitely extensible nonlinear elastic model with Peterlin's closure (FENE-P), which accounts for polymer stretching and relaxation effects as well as finite chain extensibility, allowing us to obtain in detail the behavior of the time-averaged quantities of the governing equations and their impact, contributing to the development of adequate viscoelastic closures for all drag reduction regimes. This type of analysis was initially made by Pinho *et al* (2008) and Resende *et al* (2011), with the development of a  $k-\varepsilon$  turbulent model for FENE-P fluids. They demonstrated the relevance of the various terms of the governing equations, neglecting the low impact terms, and developed new viscoelastic closures for the remaining. Those closures were developed in the context of isotropic turbulent models, and they were able to predict with good performance the behaviour for low and intermediate drag reduction regime. However the Boussinesq hypothesis started to deviate with the DR increase, because of the strong turbulence anisotropy. Therefore, the previous models were not able to predict correctly the turbulent kinetic energy evolution, and for this reason, a new model for the Reynolds stress tensor was developed that attempts to address those limitations, and is presented in this paper.

Another aspect of the turbulent model limitation to 50% DR, is related to the closure developed for the cross-correlation between the velocity gradient and tensor conformation fluctuations, designated by  $NLT_{ij}$ . To predict the anisotropy effect at high DR regimes, Iaccarino *et al* (2010) developed a  $k-\varepsilon-v^2-f$  viscoelastic turbulent model, which was able to capture this effect by  $v^2$  component, and predicted with good performance at the maximum drag reduction. Latter, this model was improved by Masoudian *et al* (2013), but in both cases the  $NLT_{ij}$  closure is not able to predict the individual components, only the trace, identical to the conformation tensor ( $C_{ij}$ ).

The evolution for better models to capture the enhanced turbulence anisotropy associated with higher levels of DR, is required, especially to capture the correct behaviour in complex geometries. Note that this effect is linked to the enhanced anisotropy of the conformation tensor, and for this reason in this paper a new viscoelastic closure is proposed for the cross correlation between the fluctuating velocity gradient and conformation tensor, essential to predict all the conformation tensor components. This closure combines an improved performance and simplicity, when compared with the previous  $NLT_{ij}$  model of Resende *et al* (2011), especially useful for the future implementation in 3D codes.

## 2. Viscoelastic closures

The governing equations for turbulent flows of viscoelastic fluids using the FENE-P constitutive equation in the context of Reynolds averaged quantities are the Reynolds-averaged continuity equation, momentum equation and a Reynolds averaged evolution equation for the conformation tensor together with an expression relating the conformation tensor with the polymer stress tensor. The momentum equation is giving by

$$\rho \frac{\partial U_i}{\partial t} + \rho U_k \frac{\partial U_i}{\partial x_k} = -\frac{\partial \bar{p}}{\partial x_i} + \eta_s \frac{\partial^2 U_i}{\partial x_k \partial x_k} - \frac{\partial}{\partial x_k} (\overline{\rho u_i u_k}) + \frac{\partial \bar{\tau}_{ik,p}}{\partial x_k}, \quad (1)$$

where  $U$  is the mean velocity,  $\bar{p}$  is the mean pressure,  $\eta_s$  is the solvent viscosity,  $\rho$  is the fluid density,  $-\overline{\rho u_i u_k}$  is the Reynolds stress tensor and  $\bar{\tau}_{ik,p}$  is the Reynolds-averaged polymer stress. Uppercase letters and overbars denote Reynolds-averaged quantities, whereas lowercase letters and primes denote fluctuations.

The Reynolds-averaged polymer stress  $\bar{\tau}_{ik,p}$  depends of the conformation tensor,  $C_{ij}$ , and is defined by the following equation

$$\bar{\tau}_{ij,p} = \frac{\eta_p}{\lambda} [f(C_{kk})C_{ij} - f(L)\delta_{ij}] + \frac{\eta_p}{\lambda} \overline{f(C_{kk} + c_{kk})c_{ij}}, \quad (2)$$

where  $\eta_p$  and  $\lambda$  are the polymer viscosity coefficient and the relaxation time of the fluid, respectively. The Peterlin functions are based on  $L^2$ , the maximum dimensionless extensibility of the model dumbbell, and are given by

$$f(C_{kk}) = \frac{L^2 - 3}{L^2 - C_{kk}} \text{ and } f(L) = 1. \quad (3)$$

The Reynolds-averaged equation describing the evolution of conformation tensor is subsequently combined with equation (2) to give equation (4), where the first-term inside the brackets on the left-hand side is Oldroyd's upper convective derivative of  $C_{ij}$ . The various terms of equation (4) have specific designations given below the horizontal brackets.

$$\left[ \underbrace{\frac{\partial C_{ij}}{\partial t} + U_k \frac{\partial C_{ij}}{\partial x_k}}_{DC_{ij}/Dt} - \underbrace{\left( C_{jk} \frac{\partial U_i}{\partial x_k} + C_{ik} \frac{\partial U_j}{\partial x_k} \right)}_{M_{ij}} \right] + \underbrace{u_k \frac{\partial c_{ij}}{\partial x_k}}_{CT_{ij}} - \underbrace{\left( c_{kj} \frac{\partial u_i}{\partial x_k} + c_{ik} \frac{\partial u_j}{\partial x_k} \right)}_{NLT_{ij}} = -\frac{1}{\lambda} ([f(C_{kk})C_{ij} - f(L)\delta_{ij}] + \overline{f(C_{kk} + c_{kk})c_{ij}}). \quad (4)$$

The contribution of  $CT_{ij}$  is neglected as previously suggested by DNS data analysis made by Pinho *et al* (2008), Resende *et al* (2011) and Masoudian *et al* (2013), for all drag reduction regimes, see Li *et al* (2006b), but the opposite occurs with the  $NLT_{ij}$  term, and for this reason

it was necessary to develop a closure. The initial closure capable to capture the  $NLT_{ij}$  behaviour at low and intermediate regimes, was developed in the isotropic context by Resende *et al* (2011). The model had an excellent performance to capture all tensor components, especially the  $uu$  component, that behaves as a production term next to the wall, and as a destructive term, away from the wall. However, the  $NLT_{ij}$  closure showed to be very complex and for this reason in the present paper we develop a new closure combining the performance factor with simplicity.

Based in the previous  $NLT_{ij}$  model of Resende *et al* (2011), the present viscoelastic closure for the  $NLT_{ij}$  term was developed taking into account future implementation in 3D codes, by reducing the number of terms and eliminating the necessity of damping functions and Weissenberg number parameter. The dependence on Weissenberg number, defined as  $Wi_{\tau_0} = \lambda u_{\tau} / \nu_0$  and based on the friction velocity,  $u_{\tau}$ , and on the zero shear-rate kinematic viscosity of the solution, i.e., the sum of the kinematic viscosities of the solvent and polymer,  $\nu_0$ , leads to simulation instabilities in complex geometries, for example turbulent flows with recirculation where the friction velocity become null, causing the well-known singularity. Resende's model, equation (5), was developed based in a compact transport equation for the exact term of the  $NLT_{ij}$  tensor derived by Pinho *et al* (2008), using the approximation given by equation (6), (more details can be found in Resende *et al* 2011).

$$\begin{aligned}
NLT_{ij} \equiv \overline{c_{kj} \frac{\partial u_i}{\partial x_k}} + \overline{c_{ik} \frac{\partial u_j}{\partial x_k}} &\approx C_{F1} \left( 0.0552 \frac{We_{\tau_0}}{25} + 0.116 \right) \times \frac{C_{ij} \times f(C_{mm})}{\lambda} \\
&- C_{F2} We_{\tau_0}^{0.743} \left[ C_{kj} \frac{\partial U_i}{\partial x_k} + C_{ik} \frac{\partial U_j}{\partial x_k} \right] + \frac{\lambda}{f(C_{mm})} \left[ C_{F3} \times \left( \frac{25}{We_{\tau_0}} \right)^{0.718} \right. \\
&\times \left( \frac{\partial U_j}{\partial x_n} \frac{\partial U_m}{\partial x_k} C_{kn} \frac{\overline{u_i u_m}}{\nu_0 \sqrt{2S_{pq} S_{pq}}} + \frac{\partial U_i}{\partial x_n} \frac{\partial U_m}{\partial x_k} C_{kn} \frac{\overline{u_j u_m}}{\nu_0 \sqrt{2S_{pq} S_{pq}}} \right. \\
&\left. \left. + \frac{\partial U_k}{\partial x_n} \frac{\partial U_m}{\partial x_k} \left( C_{jn} \frac{\overline{u_i u_m}}{\nu_0 \sqrt{2S_{pq} S_{pq}}} + C_{in} \frac{\overline{u_j u_m}}{\nu_0 \sqrt{2S_{pq} S_{pq}}} \right) \right) \right] - \frac{\lambda}{f(C_{mm})} \times f_{F1} \times C_{F4} \\
&\times \left( \frac{25}{We_{\tau_0}} \right)^{0.7} \times \left[ C_{jn} \frac{\partial U_k}{\partial x_n} \frac{\partial U_i}{\partial x_k} + C_{in} \frac{\partial U_k}{\partial x_n} \frac{\partial U_j}{\partial x_k} + C_{kn} \frac{\partial U_j}{\partial x_n} \frac{\partial U_i}{\partial x_k} + C_{kn} \frac{\partial U_i}{\partial x_n} \frac{\partial U_j}{\partial x_k} \right] \\
&\left. + \frac{\lambda}{f(C_{mm})} \left[ \frac{C_{\varepsilon_F}}{We_{\tau_0}} \frac{4}{15} \times \frac{\varepsilon^N}{(\nu_s + \nu_{\tau p}) \times \beta} C_{mm} \times f_{F2} \times \delta_{ij} \right], \tag{5}
\end{aligned}$$

$$\overline{f(\hat{c}_{mm}) c_{kj} \frac{\partial u_i}{\partial x_k}} + \overline{f(\hat{c}_{mm}) c_{ik} \frac{\partial u_j}{\partial x_k}} \approx f(C_{mm}) \left( \overline{c_{kj} \frac{\partial u_i}{\partial x_k}} + \overline{c_{ik} \frac{\partial u_j}{\partial x_k}} \right) = f(C_{mm}) NLT_{ij}. \tag{6}$$

The model is able to capture the  $NLT_{ij}$  behaviour close and away from the wall for all components, specially the negative contribution of the  $xx$  component, however as can be observed by equation (5) it is very complex with five parameters. An alternative proposed by Iaccarino *et al* (2010), relied on the turbulent viscosity normalized by the zero shear-rate kinematic viscosity of the fluid ( $\nu_T / \nu_0$ ) to capture the behaviour close to the wall, reducing the  $NLT_{ij}$  closure to one term, but it is only able to predict the trace of the  $NLT_{ij}$  tensor. The model propose here, equation (7), take into account the principle used by Iaccarino *et al* (2010) to capture the behaviour close to the wall and the capacity to predict all the individual component of the  $NLT_{ij}$  tensor achieved by Resende's model. Combining both closures it was

possible to simplify the  $NLT_{ij}$  model, reducing the number of parameters to three and the necessity to use damping functions or Weissenberg number parameters. In the development of the present model was considered the first, second and four parameters of the Resende's model ( $C_{F1}$ ,  $C_{F2}$  and  $C_{F4}$ ), equation (5), which correspond to the parameters I, II and III of the equation (7): the parameter I was modified to consider the isotropic concept by including the trace of the conformation tensor,  $C_{mm}$ , as an alternative to  $C_{ij}$ , given to the model more stability, and also was included the variation of the maximum dimensionless extensibility of the model dumbbell effect, which allowed to the closure reach high DR regime; the parameter II is the exact term of compact transport equation of  $f(\hat{c}_{mm})c_{kj}\frac{\partial u_i}{\partial x_k} + f(\hat{c}_{mm})c_{ik}\frac{\partial u_j}{\partial x_k}$  and had a direct contribution to the shear component; and the parameter III was included to give the anisotropic effect to the closure, which is simplification of the several terms involving the double velocity gradient and the tensor conformation of the parameter four present in the equation (5). In all the parameters were included the viscoelastic effect close to the wall through the Iaccarino's assumption.

$$\begin{aligned}
 NLT_{ij} \equiv & \underbrace{c_{kj}\frac{\partial u_i}{\partial x_k} + c_{ik}\frac{\partial u_j}{\partial x_k}}_I \approx \underbrace{f_N C_{N1} f(C_{mm})^{(900/L^2)} \frac{C_{mm}}{\lambda} \delta_{ij}}_I \\
 & - \underbrace{f_N^{0.35} C_{N2} \left[ C_{jk} \frac{\partial U_i}{\partial x_k} + C_{ik} \frac{\partial U_j}{\partial x_k} \right]}_{II} + \underbrace{f_N^{(1+DR^*/2.5)} C_{N3} f(C_{mm}) C_{mm}^{1.4} \frac{\frac{\partial U_i}{\partial x_k} \frac{\partial U_j}{\partial x_k}}{\sqrt{\frac{\partial U_p}{\partial x_q} \frac{\partial U_p}{\partial x_q}}}}_{III} \quad (7)
 \end{aligned}$$

with  $f_N = \nu_T/\nu_0$ . The viscoelastic parameters of the model were calibrated using DNS data for 18%, 37% and 48% DR, which belongs to low, intermediate and high regimes of DR, respectively. The DNS data present here is the same used in the development of the previous viscoelastic turbulent models of Pinho *et al* (2008), Resende *et al* (2011, 2013b), and equal to the DNS data presented by Li *et al* (2006a, 2006b), here it is possible to obtain more detailed information about the DNS methodology.

The values are:  $C_{N1} = 0.011$ ,  $C_{N2} = 0.25$  and  $C_{N3} = 1.173DR^{*-2.07}$ .

As an alternative of the  $Wi$  dependency present in many viscoelastic closures, it was introduced a  $DR^*$  parameter to the  $NLT_{ij}$  model, which is related directly to drag reduction. The  $DR^*$  parameter can be obtained by the relation developed by Li *et al* (2006a), or by equation (8). The relation of equation (8) was developed based in same principle of Li *et al* (2006a), but instead of using the typically viscoelastic parameters,  $Wi$ ,  $Re$  and  $L^2$ , related to the DR, is used the trace of conformation tensor at the wall,  $C_{kk,w}$ .

$$DR^* = 40 \left[ 1 - e^{-12.15 \left( \frac{C_{kk,w}}{900} \right)^{2.5}} \right] \left[ \left[ 1.5 - e^{-250 \left( \frac{C_{kk,w}}{2000} \right)^{2.5}} \right] \left[ 1.35 - e^{-1.1 \left( \frac{C_{kk,w}}{5000} \right)^{0.65}} \right] \right]. \quad (8)$$

The evolution of this relation can be visualized in figure 1, and compared against to the DNS data. The equation (8) is able to predict well up to 61% of DR, but for higher values the predictions starts to apart from the DNS data, reaching about 10% of error at  $DR = 75\%$ .

The Reynolds stress in equation (1) is modeled by the typically Boussinesq hypothesis through the following equation,

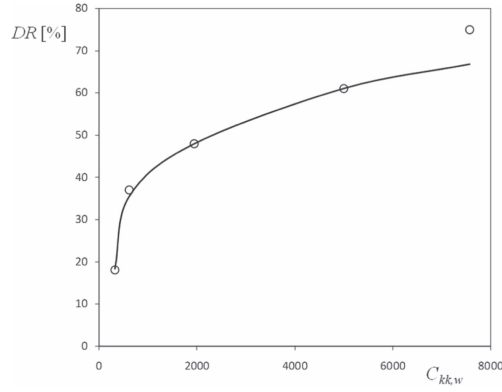


**Figure 1.** Comparison between the DR predictions (continuum line) by equation (8) based in the trace of the conformation tensor at the wall, and the DNS data (symbols) for different drag reduction regimes.

$$-\rho \overline{u_i u_j} = 2\rho(\nu_T)S_{ij} - \frac{2}{3}\rho k \delta_{ij}, \quad (9)$$

where  $S_{ij}$  is the rate of deformation tensor,  $S_{ij} = (\partial U_i / \partial x_j + \partial U_j / \partial x_i) / 2$ . The turbulent viscosity, equation (10), is defined in the isotropic context, by the typically  $k$ - $\varepsilon$  turbulent model for low Reynolds number, which was modified to capture the polymeric effect, through the trace of the conformation tensor and  $DR^*$  parameter.

$$\nu_T = C_\mu \times f_\mu \times \frac{k^2}{\varepsilon [1 + \sqrt{C_{kk}} / (24.6 \times e^{-3.1 \times DR^*})]} \quad (10)$$

with

$$C_\mu = 0.09 \text{ and } f_\mu = \left[ 1 - \exp\left(-\frac{y^+}{26.5(1 + DR^* \times 0.303 \times e^{4.93 \times DR^*})}\right) \right]^2. \quad (11)$$

The damping function  $f_\mu$  was modified to include the elastic effect close to the wall. This type of approach was first made by Cruz and Pinho (2003) using a modified GNF constitutive equation, combining the shear thinning and shear thickening rheological behaviours of the dilute polymeric solutions in the damping function, to capture the viscoelastic effect close to the wall. Latter, Tsukahara and Kawaguchi (2013) attempted the same approach, using the Giesekus model, in the development of a  $k$ - $\varepsilon$  turbulent model for viscoelastic fluids, however it failed to predict correctly the drag reduction for lower values of Weissenberg numbers and  $\beta$  ( $\beta = \nu_s / \nu_0$  is ratio between the solvent kinematic viscosity and the zero shear-rate kinematic viscosity of the fluid). In the worst case tested, the model predicted 1% of DR whereas the DNS data show 23%. Here, the damping function is linked directly to the DR to avoid this type of problem, i.e.,  $f_\mu$  is independent of the rheological parameters. The new model of  $\nu_T$  was developed using the same DNS data mention before for calibration of the  $NLT_{ij}$  closure.

### 3. Results

The performance of the new viscoelastic closure of the  $NLT_{ij}$  term and the turbulent viscosity are analyzed here through comparisons with DNS data for turbulent channel flow at the same

Reynolds number,  $Re_{\tau_0} = 395$ , which is defined by  $Re_{\tau_0} = h \cdot u_{\tau} / \nu_0$ , based on channel half-height,  $h$ , and  $\beta = 0.9$ ,  $L^2 = 900$ , and Weissenberg number of 25 and 100, equivalent to  $DR = 18\%$  and  $37\%$ , respectively. We also analyzed the effect of  $L^2$  in enhancing drag reduction for  $L^2$  between 900 and 3600 at  $Wi_{\tau_0} = 100$ .

Figures 2(a)–(c) shows the individual normal stress components of  $NLT_{ij}$  model against the previous model of Resende *et al* (2011) and DNS data, and the predictions are satisfactory good when compared with Resende’s model, with an overprediction of the  $xx$  component close to wall for intermediate and high regimes of DR, where its acts as a production term, and at the log-law region, for low and intermediate DR regimes. The maximum deviation of the peak value is about 3.5% at  $DR = 48\%$ , and 22% for the previous model at  $DR = 37\%$ , when compared with DNS data. The behaviour of previous model for high regime of DR is not presented due to the limitation of the  $k$ - $\varepsilon$  turbulent model to intermediate DR regime, where the saturation effect of the viscoelastic phenomenon is achieved at  $DR = 43.8\%$  (see figure 21 of Resende *et al* 2011). In the previous model the predictions start apart from the DNS data as we increase DR, in terms of the peak value and its location, as can be observed for  $DR = 37\%$ .

For the  $yy$  component, there is a small overprediction away from the wall, and an underprediction close to the wall for low regime of DR, but at high regime of DR it can be observed an 17% overprediction of the maximum value, in contrast with the previous model where it is possible to visualize a 25% underprediction for intermediate regime of Dr. In case of  $zz$  component there is an underprediction for all regimes, consequence of the development of NLT model in the isotropic context. Nevertheless, for all three components the increase of the maximum value and its shift away from the wall was captured by the present model, where the previous model fails. Although the lower accuracy of the  $zz$  component predictions, the impact is very low, as shows the trace of the  $NLT_{ij}$  tensor, figure 2(d). The  $NLT_{kk}$  behaviour is also satisfactory predicted, with a small underprediction in the buffer layer zone, resulting of the  $zz$  component underprediction. Close to the wall, the  $NLT_{kk}$  present similar behaviour of the  $xx$  component. In all DR regimes, the predictions capture the increase of the maximum value of  $NLT_{kk}$  with drag reduction and its shift away from the wall, where the previous model diverge with an 23% underprediction of the peak value at intermediate regime of DR, against 4.5% error obtained by the present model. The evolution of the shear component of  $NLT_{ij}$  by the present closure can be visualize in figure 2(e), keeping the same accuracy present before for the others components, where in all cases the maximum value increased and its shift away from the wall with DR, as expected, with a maximum deviation error of 7%. The previous model is not able to capture correctly the shear component behaviour, showing a significant deviation from the DNS data with an 120% and 35% overprediction of the maximum value in case of 18% and 37% DR, respectively.

Overall, this new closure of  $NLT_{ij}$  had a better performance than the previous closure for  $DR = 18\%$  and  $37\%$ , and is significantly simpler.

Figure 3 compares the prediction of the new turbulent viscosity, equation (10), with the results of DNS simulations for all DR regimes,  $DR = 18\%$ ,  $37\%$  and  $48\%$ , corresponding to low, intermediate and high DR, respectively. The new model is able to capture the elastic effect with good performance, where the predictions coincide with the DNS data. It was also included the predictions of Resende’s model for comparison (details of the previous turbulent viscosity closure can be found in Resende *et al* 2011), and it can be observed that the previous model had similar behaviour close to the wall, diverging significantly from the DNS data for  $y^+ > 130$ . In all cases the maximum value and its location are well predicted, with the DR increase. Consequently, the



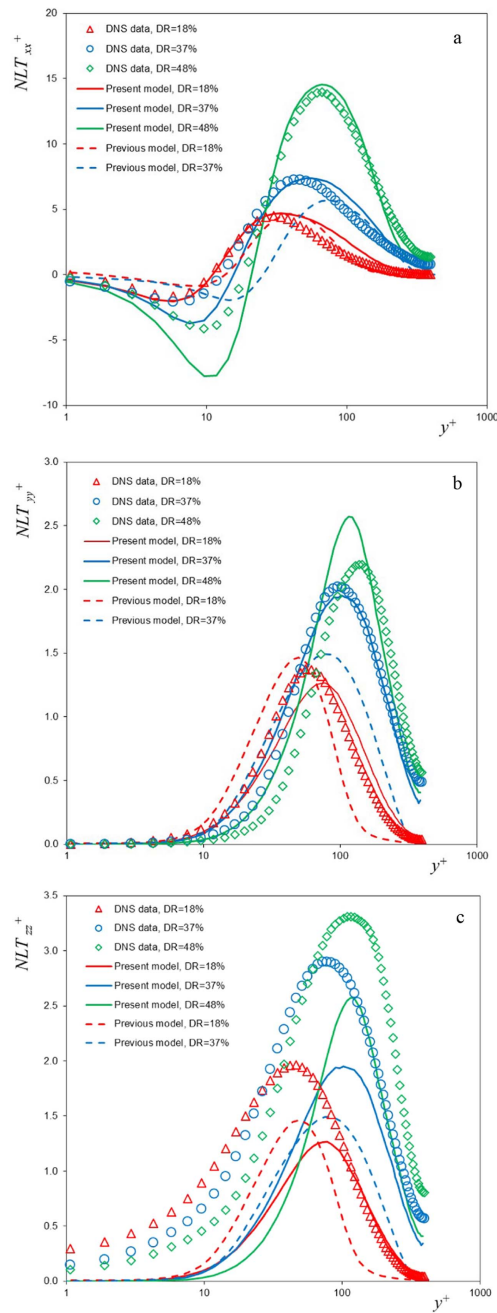


**Figure 2.** Comparison between the  $NLT_{ij}^+$  model predictions of the individual components (continuum lines —), ((a)— $xx$  component; (b)— $yy$  component; (c)— $zz$  component; (d)—trace of  $NLT_{ij}$ ; (e)— $xy$  component), previous model of Resende *et al* (2011) (dash lines - -) and the DNS data (symbols) for  $Re_{\tau 0} = 395$  and  $\beta = 0.9$  at different drag reduction regimes: (1) DR = 18%:  $L^2 = 900$  and  $Wi_{\tau 0} = 25$ ; (2) DR = 37%:  $L^2 = 900$  and  $Wi_{\tau 0} = 100$ ; (3) DR = 48%:  $L^2 = 3600$  and  $Wi_{\tau 0} = 100$ .

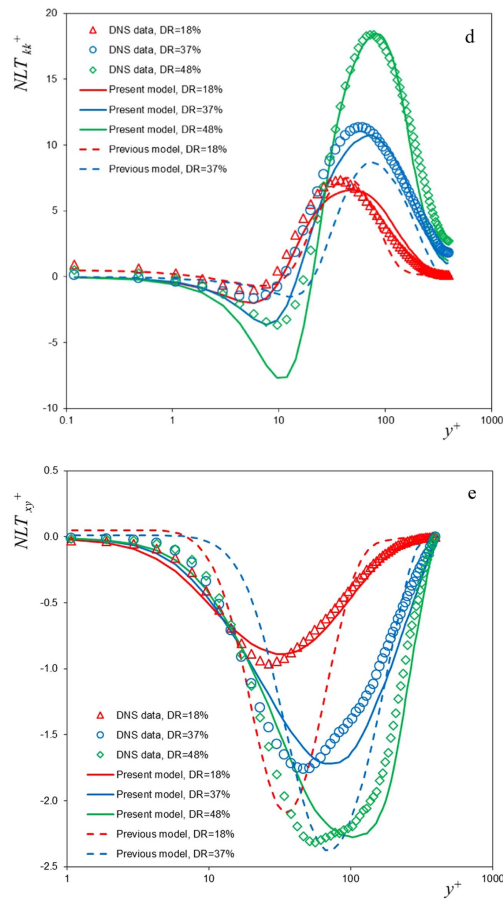
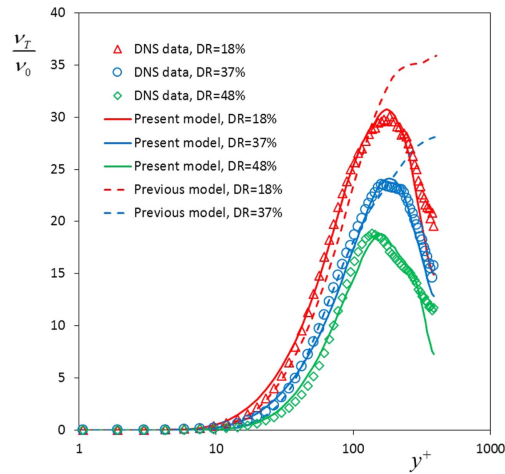


Figure 2. (Continued.)

production of  $k$ ,  $P_k = -\rho \overline{u_i u_j} \partial U_i / \partial x_j$ , is also well captured, as can be visualized in figure 4, except close to the wall where there is an overprediction due to a very small increase of the turbulent viscosity predictions for  $y^+ < 60$ . This demonstrates the impact of the model performance to predict the turbulent kinetic energy correctly, referenced also by Resende *et al* (2014), where it is shown that an underprediction of  $P_k$  originates a wrong behaviour of  $k$ , and a decrease of  $k$  as DR increases. Resuming, the overprediction of  $P_k$  by the new turbulent viscosity closure, will allow to increase  $k$  as DR increases, correcting the fail of the previous isotropic viscoelastic turbulent models.

#### 4. Conclusions

The new viscoelastic closure developed for the  $NLT_{ij}$  tensor is able to capture satisfactorily all its components when compared with DNS data, but the main advantage of the present model is its simplicity, which allows its easy implementation in 3D codes. This closure is able to capture the negative contribution of the  $xx$  component close to the wall, similar to the model developed by Resende *et al* (2011). However, it is very complex, containing up to five parameters, but in this case it was possible to reduce these just to three. Another major advantage



**Figure 3.** Comparison between the predictions of turbulent viscosity model, equation (10), (continuum lines —), previous model of Resende *et al* (2011) (dash lines - -) and the DNS data (symbols) for  $Re_{\tau_0} = 395$  and  $\beta = 0.9$ , at different drag reduction regimes: (1) DR = 18%:  $L^2 = 900$  and  $Wi_{\tau_0} = 25$ ; (2) DR = 37%:  $L^2 = 900$  and  $Wi_{\tau_0} = 100$ ; (3) DR = 48%:  $L^2 = 3600$  and  $Wi_{\tau_0} = 100$ .

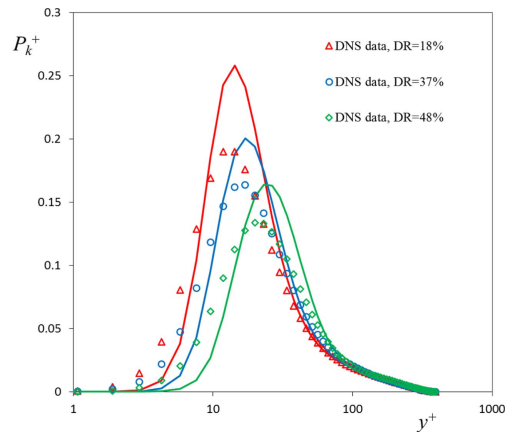


**Figure 4.** Comparison between the predictions of turbulent production of  $k$ ,  $P_k$ , (continuum lines) and the DNS data (symbols) for  $Re_{\tau_0} = 395$  and  $\beta = 0.9$ , at different drag reduction regimes: (1) DR = 18%:  $L^2 = 900$  and  $Wi_{\tau_0} = 25$ ; (2) DR = 37%:  $L^2 = 900$  and  $Wi_{\tau_0} = 100$ ; (3) DR = 48%:  $L^2 = 3600$  and  $Wi_{\tau_0} = 100$ .

of this new closure is the absence of damping functions, i.e., the new closure is independent of wall distance, typically used in low Reynolds number models.

Previous isotropic turbulence models for FENE-P fluids showed a deficit of  $k$  and this was traced to a deficit in the production of  $k$ . In this work a modification is made to the closure for the Reynolds stress that corrects that deficiency. This modification consist in the introduction of a polymeric contribution to the turbulent viscosity, which is based on the trace of the conformation tensor and DR parameter, both independent of wall distance.

Finally, a new relation is developed to predict DR based only on the trace of the conformation tensor at the wall, an alternative to the relation of Li *et al* (2006a), which depends of three parameters: the  $Wi$  and  $Re$  numbers, and  $L^2$ .

The main advantage of the closure proposed here is the combination of the performance with simplicity, allowing future developments of new isotropic turbulent models, with FENE-P fluids, for complex geometries.

## Acknowledgments

Financial support provided by CNPq—Conselho Nacional de Desenvolvimento Científico e Tecnológico through Project N° 449361/2014-4 and FAPESP—Fundação de Amparo à Pesquisa do Estado de São Paulo is gratefully acknowledged by P R Resende.

## References

- Cruz D O A and Pinho F T 2003 Turbulent pipe flow predictions with a low Reynolds number  $k$ - $\varepsilon$  model for drag reducing fluids *J. Non-Newton. Fluid Mech.* **114** 109–48
- Cruz D O A, Pinho F T and Resende P R 2004 Modeling the new stress for improved drag reduction predictions of viscoelastic pipe flow *J. Non-Newton. Fluid Mech.* **121** 127–41
- Dubief Y, Terrapon V E and Soria J 2013 On the mechanism of elasto-inertial turbulence *Phys. Fluids* **25** 1–16
- Iaccarino G, Shaqfeh E S and Dubief Y 2010 Reynolds-averaged modeling of polymer drag reduction in turbulent flows *J. Non-Newton. Fluid Mech.* **165** 376–84
- Li C F, Gupta V K, Sureshmar R and Khomami B 2006a Turbulent channel flow of dilute polymeric solutions: drag reduction scaling and an eddy viscosity model *J. Non-Newton. Fluid Mech.* **139** 177–89
- Li C F, Sureshmar R and Khomami B 2006b Influence of rheological parameters on polymer induced turbulent drag reduction *J. Non-Newton. Fluid Mech.* **140** 23–40
- Masoudian M, Kim K, Pinho F T and Sureshkumar R 2013 A viscoelastic  $k$ - $\varepsilon$ - $v^2$ - $f$  turbulent flow model valid up to the maximum drag reduction limit *J. Non-Newton. Fluid Mech.* **202** 99–111
- Pinho F T 2003 A GNF framework for turbulent flow models of drag reducing fluids and proposal for a  $k$ - $\varepsilon$  type closure *J. Non-Newton. Fluid Mech.* **114** 149–84
- Pinho F T, Li C F, Younis B A and Sureshkumar R 2008 A low Reynolds number  $k$ - $\varepsilon$  turbulence model for FENE-P viscoelastic fluids *J. Non-Newton. Fluid Mech.* **154** 89–108
- Resende P R, Escudier M P, Presti F, Pinho F T and Cruz D O A 2006 Numerical predictions and measurements of Reynolds normal stresses in turbulent pipe flow of polymers *Int. J. Heat Fluid Flow* **27** 204–19
- Resende P R, Kim K, Younis B A, Sureshkumar R and Pinho F T 2011 A FENE-P  $k$ - $\varepsilon$  turbulence model for low and intermediate regimes of polymer-induced drag reduction *J. Non-Newton. Fluid Mech.* **166** 639–60
- Resende P R, Pinho F T and Cruz D O A 2013a A Reynolds stress model for turbulent flows of viscoelastic fluids *J. Turbul.* **14** 1–36
- Resende P R, Pinho F T, Kim K, Younis B A and Sureshkumar R 2013b Development of a low-Reynolds-number  $k$ - $\omega$  model for FENE-P fluids *Flow Turbul. Combust.* **90** 69–94
- Resende P R, Pinho F T and Oliveira P J 2014 *5th National Conf. on Fluid Mechanics, Thermodynamics and Energy—MEFTE* (Porto, Portugal) pp 221–6
- Tsukahara T and Kawaguchi Y 2013 Proposal of damping function for low-Reynolds-number  $k$ - $\varepsilon$  model applicable in prediction of turbulent viscoelastic-fluid flow *J. Appl. Math.* **2013** 1–15